Supplementary Information:

3D Flexible Water Channel: Stretchability of Nanoscale Water Bridge

Jige Chen, Chunlei Wang, Ning Wei, Rongzheng Wan, and Yi Gao

I. Capillary Stability of the Water Bridge

The capillary stability of the nanoscale water bridge could be presented by two nanoscale characteristics, (1) the average potential energy of water molecules, E_p, and (2) the molecule density of the water bridge, D_N, to characterize the capillary stability. They can be calculated as,

$$E_p = \sum E_p / N , \qquad D_N = N / l_B \qquad \text{(S1)}$$

where E_p is the potential energy of water molecule within the water bridge, and N is the water molecule number, and l_B is the length of the water bridge. Therefore E_p could refer to the water bridge stability from the perspective of structural energy, while D_N could refer to water bridge stability from the perspective of molecular organization.

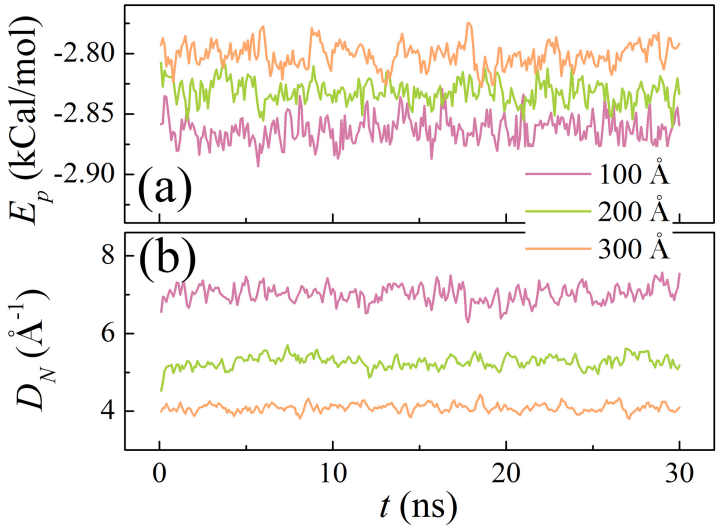

Fig. S1 Time variations of (a) E_p and (b) D_N for the nanoscale water bridge with length l_B=100, 200, 300 Å in 30 ns.

We carry out additional MD simulations to investigate the two characteristics in the water bridges that are stretched to be 100, 200, and 300 Å. In Fig. S1, we illustrate the

time variations of both E_p and D_N for the nanoscale water bridges in 30 ns. It shows that, in the simulation timescale, the two characteristics maintain a steady variation. For example, for the water bridge with a length to be 200 Å, its average potential energy E_p fluctuates around -2.83 kCal/mol, and its density D_N flucates around 5.27 $Å^{-1}$.

II. Molecular Organization

The molecular organization of water layer in the water bridge differs from the bulk part on the solid plate. To make a comparison of them, we investigate the distribution of E_p and D_N to understand the microscopic structural variance of the water bridge.

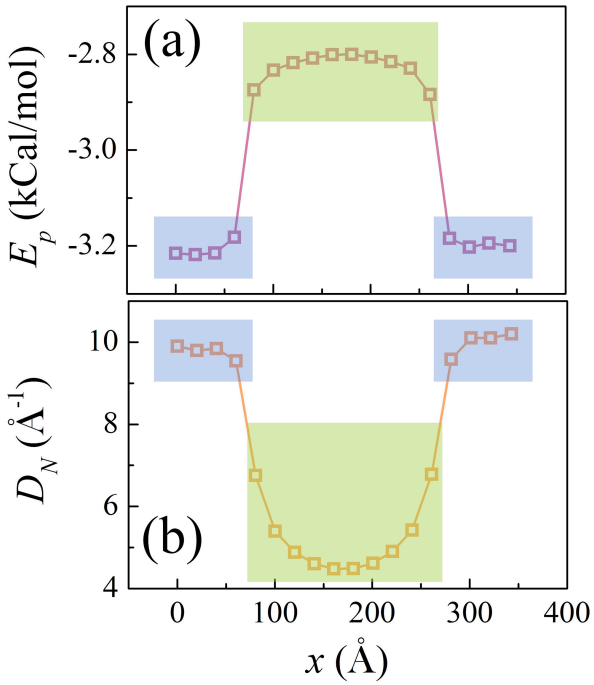

Fig. S2 Distribution of (a) E_p and (b) D_N along the nanoscale water bridge with length l_B=200 Å (covered by the green squares), and along the separated plate (covered by the blue squares).

The distribution of E_p and D_N are illustrated in Fig. S2. Here we divide the water layer into 18 slabs, which is 20 Å long in each slab, to compute the value of E_p and D_N by Eq. S1 in the above response. The inner 10 slabs correspond to the water bridge and the outmost 8 slabs correspond to the water layer on the solid plate. Comparing with

the bulk part of water layer on the plate, water molecules in the water bridge exhibit much higher potential energy. The maximum value E_p= -2.80 kCal/mol is observed in the central part of the water bridge, which implies the most intensified part by stretching. Meanwhile, the molecule density of the water bridge is significantly decreased in the water bridge. It is reduced to D_N=4.47 Å^{-1} in the central position, which is far most far away part from the plate.

III. Molecular Organization Variation in Stretching

To characterize the molecular organization of the water bridge upon the electric field in the stretching, we have considered the molecule number ratio R in the water bridge in Fig. 2(a). Since E_p and D_N also refer to the molecular organization of the water bridge, thus we would like to consider their variations in stretching. In the following, we shall clarify the advantage of choosing R, instead of E_p or D_N, to describe the variation of molecular organization in stretching.

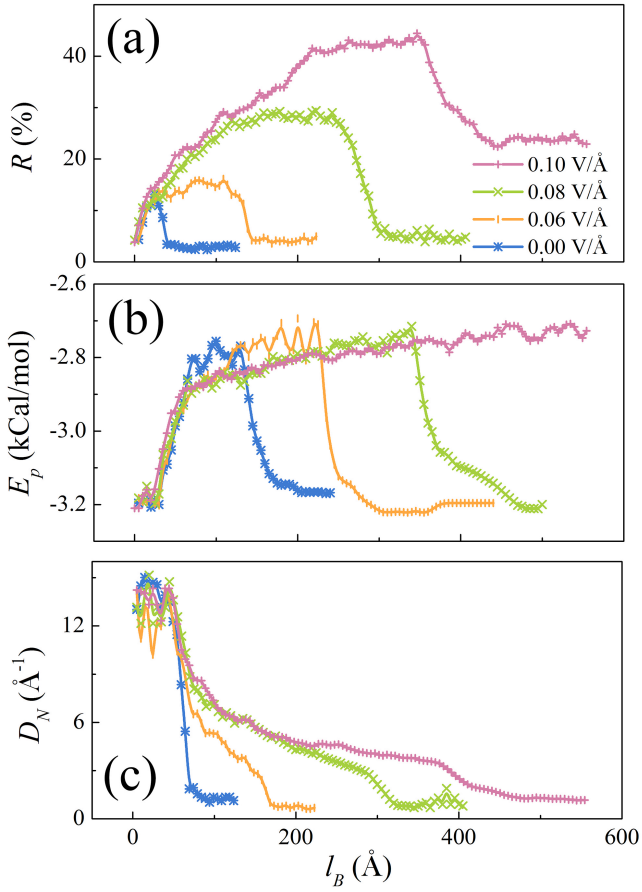

Fig. S3 Variations of (a) the molecule number ratio R, and (b) average potential

energy E_p and (c) molecule density D_N of the water bridge in its formation-to-breaking process under different electric field magnitude.

As shown in Fig. S3(a) and Fig. 2(a) in the manuscript, the three stages in the formation-to-breaking process of the water bridge, i.e., the stretching, holding, and breaking, can be easily distinguished by investigating the variation of R. Therefore, it provides a clear way to observe the molecular organization variation under different electric field in stretching.

On the other hand, as shown in Fig. S3(b), by investigating the variations of E_p, the three stages could still be observed. However, E_p is lagging behind the variation of molecular organization of the water bridge. The reason of such delay is due to the gradually relaxation of potential energy, which is insufficient to represent a sudden change of the water bridge structure in real time. For example, for E=0.08 V/ Å, the water bridges breaks at l_B=320 Å, but E_p drops down only until l_B=360 Å, which means 40 Å delay in the presentation of E_p.

Meanwhile, as shown in Fig. S3(c), by investigating the variations of D_N, the three stages could not be clearly presented. For example, for E=0.08 V/ Å, in the initial stretching stage, D_N exhibits a strong fluctuation since the water bridge length l_B is too small. In the breaking stage, D_N becomes very small when l_B increases, thus it is quite difficult to distinguish it from the holding stage.

IV. First Arrive Time of the LJ Particle

The diffusion behavior of the LJ particle in the water bridge might be affected by the interaction strength between the LJ particle and the water molecules, and the size of the LJ particle. Therefore, we intend to investigate the first arrive time of the LJ particle from the left to the right part of the water bridge, by varying its ε which refers to the interaction strength, and σ which refers to the particle size.

The MD simulations start from the same initial condition in Fig. 5, with different LJ parameters ε and σ. Since the simulation of the diffusion of the LJ particle is very time-consuming, thus we carry out 4 (4×5 = 20 in total) independent simulations in

each case for a qualitative result.

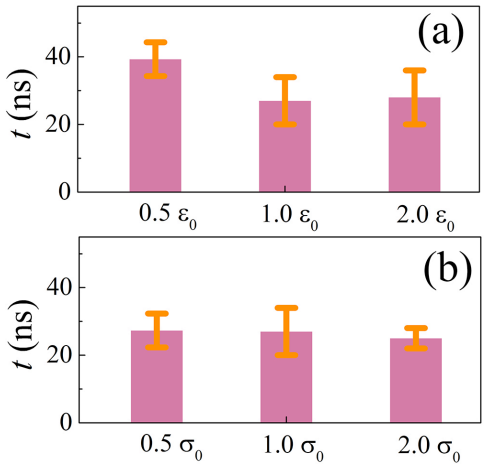

Fig. S4 The first arrive time of the LJ particle, *t,* to reach the other side of the water bridge by varying the LJ parameters (a) ε and (b) σ.

As shown in Fig. S4(a), the weakest interaction $0.5\varepsilon_0$ refers to a much long first arrive time than both ε_0 and $2\varepsilon_0$. It suggests that the weak interaction would slow the spontaneous diffusion of the LJ particle in the water bridge. Meanwhile, as shown in Fig. S4(b), the first arrive time of the LJ particle exhibits no observable differences by varying the value of σ. It implies that the diffusion of a single LJ particle is not very sensitive to its particle size.